Oscillator Strengths of Ca II, Sr II, and Ba II

ALAN GALLAGHER*
Joint Institute for Laboratory Astrophysics,† Boulder, Colorado
(Received 28 October 1966)

The lifetimes of the $5p^2P_{3/2}$ and $5p^2P_{1/2}$ states of Sr^+ and the $6p^2P_{3/2}$ and $6p^2P_{1/2}$ states of Ba^+ have been measured by the Hanle-effect technique with optical excitation from the ion ground state. (The lifetimes of the Mg^+ $3p^2P_{3/2}$ and Ca^+ $4p^2P_{3/2}$ states were obtained by the same technique and reported previously.) These Ca^+, Sr^+, and Ba^+ states each decay to a $^2D_{3/2,5/2}$ doublet as well as to the ground $^2S_{1/2}$ state, and the branching ratios for these transitions have been measured. The ions were produced by introducing traces of the atomic vapor into an argon discharge. Consequently, the cross sections for collisional depolarization of these ^2P_J states due to collisions with argon were also obtained from the measurements. The experimental results are given in Tables I and II. A discussion of the ion-atom collisional depolarization cross sections is included.

INTRODUCTION

THE Hanle-effect measurements reported here utilize techniques that were developed by Smith[1] and the author while Smith was at this laboratory. We have already reported these techniques in considerable detail, along with our results for the $Mg^+3p^2P_{3/2}$-state and $Ca^+4p^2P_{3/2}$-state lifetimes.[2] Consequently, only a brief description of our methods appears here, along with discussions of a few special features that enter into the Sr^+ and Ba^+ Hanle-effect measurements.

Some of the transition probabilities reported here have been measured by the hook method,[3] by arc methods,[4] and recently by the Hanle-effect method.[5] Uncertainties in arc results are much larger than those of the present experiments. The hook measurements are assigned an uncertainty of about $\pm 30\%$, while the present experiments have (4–10%) uncertainties for the same transitions. Since the major part of this hook method uncertainty is due to the uncertainty in the ion density, the hook ratios of $ns^2S_{1/2}$-$np^2P_{1/2,3/2}$ transition probabilities from a common ground state provide a check on the present results. The Hanle-effect measurement of the Ba^+ $6p^2P_{3/2}$-state lifetime is assigned an accuracy of $\pm 9\%$.[5] The lifetime measurements reported here are assigned uncertainties of $\pm 3\%$ to $\pm 5\%$, while the branching ratio accuracies are $\pm 10\%$ to $\pm 20\%$. These accuracies are sufficient to afford a useful test of present theoretical results, and comparisons with the other experimental results and with theories are included with the conclusions.

The group-II*A* ions studied here have a primarily single-electron structure with a $ns^2S_{1/2}$ ground state. The metastable $(n-1)d$ state and the np state form the first two excited doublets in all but the Mg^+ case where $n-1=2$ and the d state does not occur. The lifetimes reported here are those of the np doublet states, while the branching ratios are those for the np-ns versus np-$(n-1)d$ decay transitions.

The Ca^+ and Mg^+ ns-np doublet lines could not be separated in these experiments without considerable loss of intensity, but the $np^2P_{3/2}$-state lifetime can be obtained without separating the lines since linearly polarized light produces a Hanle effect in the $J=\frac{3}{2}$ state but not in the $J=\frac{1}{2}$ state. The small doublet separations would lead one to expect at most a few percent difference between the $np^2P_{3/2}$- and $np^2P_{1/2}$-state lifetimes, and this expectation is partially verified by hook ratio measurements for Ca^+.[3,6] Consequently, no measurements of the Mg^+ and Ca^+ $np^2P_{1/2}$-state lifetimes were attempted. Equivalent arguments for the Ca^+ np-$(n-1)d$ transitions have been used to relate the branching ratios from the Ca^+ $np^2P_{3/2}$ and $np^2P_{1/2}$ states, so that only one ratio measurement of the unresolved Ca^+ doublet lines was made. In Sr^+ and Ba^+ the np doublet separation is large enough to produce considerable difference between the $np^2P_{3/2}$- and $np^2P_{1/2}$-state lifetimes and branching ratios, and at the same time it is large enough to allow the use of a wide angle interference filter to separate the pumping lines. Consequently the lifetimes and branching ratios of the $np^2P_{3/2}$ and $np^2P_{1/2}$ states were measured separately for Sr^+ and Ba^+.

Since the scattering ions were produced in an argon discharge in these experiments, the ion excited states were partially depolarized (during the excited-state lifetime) by collisions with argon. This caused a decrease in the magnitude of the Hanle-effect signal and a decrease in the measured lifetime, so that it was essential to operate at argon pressures where this depolarization (of magnitude $n\bar{v}\sigma\tau$) was a fairly small effect. Since σ was found to be on the order of 10^{-14} cm^2, and since the life-

* This research was supported by the National Science Foundation under Grant No. GP-5191.

† Of the National Bureau of Standards and University of Colorado, Boulder, Colorado.

[1] Present address: Columbia University, New York, New York.

[2] Winthrop W. Smith and Alan Gallagher, Phys. Rev. **145**, 26 (1966).

[3] Yu. I. Ostroskii and N. K. Penkin, Opt. i. Spektroskopiya **10**, 8 (1960); **11**, 565 (1961) [English transls.: Opt. Spectry. (USSR) **10**, 3 (1961); **11**, 307 (1961)].

[4] C. H. Corliss and W. R. Bozman, Natl. Bur. Std. (U.S.) Monograph 53 (1962).

[5] H. Bucka, J. Eichler, and G. v. Oppen, Z. Naturforsch. **21**, 654 (1966).

[6] E. I. Nikonova and V. K. Prokofiev, Opt. i. Spektroskopiya, **1**, 290 (1956).

times were $\sim 10^{-8}$ sec, this condition was satisfied at argon pressures in the 0.05–1.0 Torr range. In this pressure range cold-cathode discharges are very effective ionizers, so that ion densities large enough to give multiple scattering of the ion resonance radiation were easily produced. The applicability of the present methods of ion production to the measurement of other ion-excited-state lifetimes thus depends on the excited-state lifetime and on the collisional depolarization cross section in each case. For this reason, as well as for the desirability of understanding the principal depolarization mechanism, an extension of the theories of atom-atom depolarizing collisions[7–9] to the present ion-atom case is presented in Appendix III. The conclusion reached is that about 10^{-14} cm^2 depolarizing cross sections can be expected for most ion excited states, with certain exceptions that also cause different cross sections in atom-atom collisions.

THE HANLE-EFFECT EXPERIMENTS

The methods used to measure the ion Hanle effects are described in detail in Ref. 2, but will be briefly reiterated here. The scattering ions are produced by spraying traces of the atomic vapor into a pulsed argon discharge. The scattered-ion resonance radiation is detected after the discharge is off and collisional depolarization of the ion excited state by discharge products has become negligible. The radiation is scattered 90° in the plane perpendicular to the magnetic field. The incident and detected radiation are linearly polarized (in the scattering plane) for the $np^2P_{3/2}$-state measurements, and circularly polarized for the $np^2P_{1/2}$-state measurements. In both cases the field dependence of the number of ions produced by the discharge is detected by scattering π polarized radiation.

Using this information, the measured Hanle-effect signal shapes are corrected for the changing number of ions. The $np^2P_{3/2}$-state Hanle-effect signal shape is $(1+x^2)^{-1}$ where $x=4\pi g_{3/2}\mu_0 H\tau/h$, and the $np^2P_{1/2}$-state signal shape is $y(1+y^2)^{-1}$ where $y=2\pi g_{1/2}\mu_0 H\tau/h$. Once the magnetic field dependence was found to be Lorentzian, the linewidth data were obtained with field modulation and lock-in detection. The linewidths were taken from the zeros of the second harmonic for the $np^2P_{3/2}$-state measurements and of the first harmonic for the $np^2P_{1/2}$ states (with a few percent modulation correction in each case).

Since multiple photon scattering narrows the measured Hanle-effect linewidths, the limiting width at zero ion density is found at each argon pressure. These limiting linewidths are plotted against argon pressure to obtain the natural width and the argon collisional depolarization cross sections (Fig. 1). The results are given in Table I. The percentage uncertainties in the $^2P_{1/2}$-state lifetimes are larger than those for the $^2P_{3/2}$ states because the gradual field dependence of the discharge generally produced a greater distortion of the larger $^2P_{1/2}$-state linewidths.

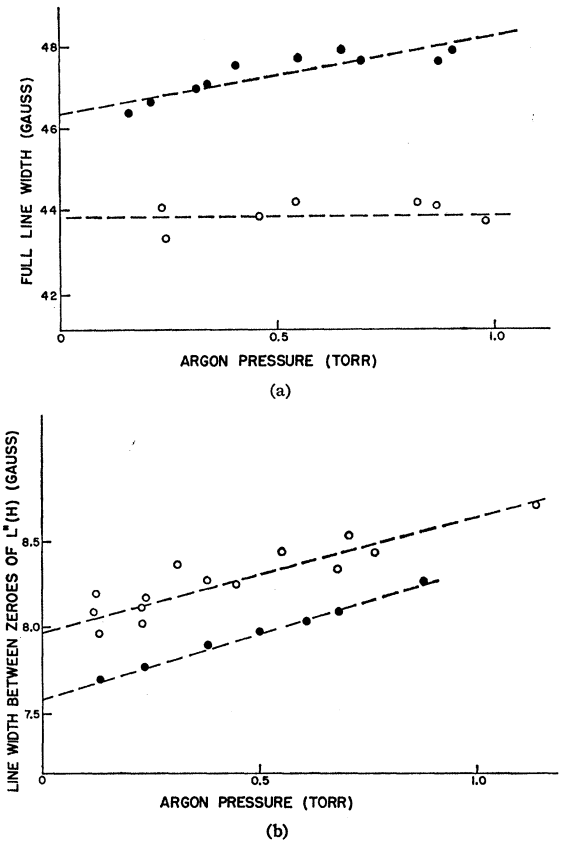

FIG. 1. Hanle-effect linewidths from (a) $np^2P_{1/2}$ states (b) $np^2P_{3/2}$ states. Open circles are Ba^+ data; dots are Sr^+ data. The 2–5% modulation broadening correction has already been applied to the actual data. The limit of zero ion optical depth has been used at each argon pressure.

Other experimental details such as signal symmetrization and lamp-profile checks were carried out as discussed in Ref. 2. One additional complication which enters the Ba^+ measurements is the effect of the $I=\frac{3}{2}$ isotope scattering signal (natural abundance 18%). The Ba^+ $6s^2S_{1/2}$-state hyperfine structure (hfs) of 0.25 cm^{-1} will probably separate the odd-isotope resonance lines from those of the even isotopes by slightly more than the Doppler width of the lamp, so that one would expect somewhat less than 18% odd-isotope excitation by a lamp that is free from self-reversal. However, the percentage of odd-isotope scattering was indirectly measured in the branching ratio experiment and found to be near 20%. It is shown in Appendix I that this percentage of odd isotope scattering would cause about 1.5% broadening of the modulation detected ($I=0$) $6p^2P_{3/2}$-state linewidth and a negligible broadening to the

[7] F. W. Byron, Jr. and H. M. Foley, Phys. Rev. 134, A625 (1964).
[8] A. Omont, J. Phys. Radium 26, 26 (1965).
[9] M. I. D'Yakonov and V. I. Perel, Zh. Eksperim. i Teor. Fiz. 48, 345 (1965) [English transl.: Soviet Phys.—JETP 21, 227 (1965)].

TABLE I. Experimental results.[a]

State	Lifetime (10^{-9} sec)	Branching ratio $\left(\frac{A(^2P-^2S_{1/2})}{\sum_J A(^2P-^2D_J)}\right)$	Argon collision depolarization cross sections at ~140°C (10^{-14} cm^2)
Mg^+ $3^2P_{3/2}$	3.67±0.18[b]	Does not branch	1.3 ±0.25[b]
Ca^+ $4^2P_{3/2}$	6.72±0.2[b]	17.6 ±2[c]	1.4 ±0.2[b]
Sr^+ $5^2P_{3/2}$	6.53±0.2	14.8 ±2.5	1.2 ±0.25
Sr^+ $5^2P_{1/2}$	7.35±0.3	13.4 ±2	0.47±0.25
Ba^+ $6^2P_{3/2}$	6.27±0.25	2.85±0.3	1.25±0.25
Ba^+ $6^2P_{1/2}$	7.74±0.4	2.77±0.3	0.0 ±0.25

[a] The quoted errors represent an attempt to safely allow for systematic error; standard deviations of the mean were negligible in comparison.
[b] These results were previously reported in Ref. 2.
[c] A combination of $4^2P_{1/2}$ and $4^2P_{3/2}$ branching was measured for Ca^+ (see text for analysis).

($I=0$) $6p^2P_{1/2}$-state linewidth. This 1.5% correction was used to obtain the $6p^2P_{3/2}$-state lifetime, and an additional 1% was included in the uncertainty. The 7% of $I=\frac{9}{2}$ isotope in natural strontium has an insignificant effect on the Sr^+ linewidths.

THE BRANCHING-RATIO EXPERIMENTS

The branching ratios for the np-ns versus np-$(n-1)d$ decay modes were obtained by measuring the ratio of intensities fluoresced into each mode by the optically pumped ions. The limiting ratios at zero ion density were obtained, since radiation trapping of the np-ns photons will cause the proportion of np-$(n-1)d$ photons reaching the detector to exceed the natural ratio (see Fig. 2 for an example of the data). The same lamp and pulsed discharge scattering chamber were used, with unpolarized radiation scattered 90° in the plane perpendicular to a dc magnetic field. An interference filter between the lamp and scattering chamber isolated the $ns^2S_{1/2}$-$np^2P_{1/2}$ or $ns^2S_{1/2}$-$np^2P_{3/2}$ resonance line from the remainder of the lamp spectrum. Glass absorption filters were used between the scattering chamber and photomultiplier to alternately block the radiation of the np-ns or np-$(n-1)d$ decay modes. In all cases the $(n-1)d$ doublet separation is quite small, and we see no reason to suspect that the σ^2 for the $np^2P_{3/2}$-$(n-1)d^2D_{3/2}$ and $np^2P_{3/2}$-$(n-1)d^2D_{5/2}$- transitions should differ significantly. Consequently both $np^2P_{3/2}$-$(n-1)d^2D_J$ lines were simultaneously detected, and it was assumed that the intensity ratio of the doublet lines corresponded to equal σ^2 values. (It follows that $A(^2P_{3/2}$-$^2D_{5/2})/A(^2P_{3/2}$-$^2D_{3/2})\cong 9$, so it was primarily $A(^2P_{3/2}$-$^2D_{5/2})$ that was measured in these experiments.)

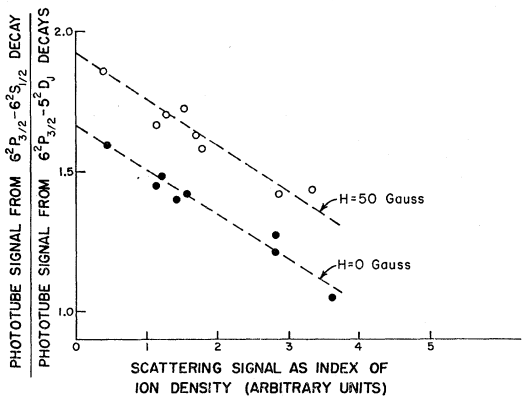

FIG. 2. Ba^+ $6p^2P_{3/2}$-state branching-ratio measurements.

The relative spectral sensitivity of an S-1 photomultipler was calibrated by comparing its sensitivity to that of a lampblack-coated Eppley thermopile, which has a flat response across the 0.39- to 1.1-μ range investigated. This was done by filtering light from xenon arc and tungsten ribbon sources with two monochromators in series, and imaging the final monochromator slit onto the thermopile (mirror lenses were used in the second monochromator and final imaging so that the imaging was independent of wavelength). The photomultiplier was interposed in the converging beam to intercept all of the radiation incident on the thermopile but at a position where it was spread out over the photocathode (in the ion fluorescence measurements the radiation was also detected with almost the entire cathode area). Generally, the accuracy of this relative sensitivity calibration should be near 5%, but the np-$(n-1)d$ lines of Sr^+ are between 1.0 and 1.1 μ where the photocathode sensitivity is dropping rapidly and some loss of accuracy is expected for these wavelengths.

The decay radiation from the optically pumped $^2P_{1/2}$ states is isotropic and unpolarized, so that the measured np-$(n-1)d$ versus np-ns intensity ratio multiplied by the photon wavelength ratio will be the desired ratio of transition probabilities. The decay radiation from the optically pumped $^2P_{3/2}$ states will not be isotropic (for any magnetic field), and the relative anisotropy will be different for the np-ns versus np-$(n-1)d$ decay modes. Consequently, the ratio measurements for the $^2P_{3/2}$ decays were made with 0 and 50 G magnetic fields ($4\pi g_J\mu_0 H\tau/h \gg 1$ at 50 G), and these ratios were related to the np-ns and np-$(n-1)d$ transition probabilities with the Breit resonance fluorescence formula[10,11] (details of the calculation are given in Appendix II). The conclusion reached in Appendix II is that when $H=\infty$, a 5% greater proportion of the np-ns decay radiation

[10] G. Breit, Rev. Mod. Phys. **5**, 91 (1933).
[11] P. Franken, Phys. Rev. **121**, 508 (1961).

compared to the np-$(n-1)d$ radiation is scattered into the detector. At $H=0$ a 13% larger proportion of the np-$(n-1)d$ radiation compared to the np-ns radiation is received by the detector. Thus the intensity ratios with $H=0$ and $H=\infty$ should differ by 18%. The Sr^+ ratios at $H=0$ and $H=50$ G differed by about (16±1)%, indicating that about 10% of the scattering was isotropic from the $I=\frac{7}{2}$ isotope (9% abundant). The Ba^+ ratios at $H=0$ and $H=50$ G differ by (15±1)%, indicating that about one-sixth of the scattering was virtually isotropic from the odd isotopes (natural abundance 18%). This information was therefore used to make a small correction for the actual anisotropy. In the Ca^+ case the interference filter did not isolate the $4p^2P_{1/2}$- and $4p^2P_{3/2}$-state resonance lines, so that the combined $4p$-$3d$ decay intensities from both $4p$ states were compared to the combined $4p$-$4s$ intensities. In Ca^+, however, the $4p$ doublet separation is so small that it can be reasonably assumed that the σ^2 values for the $4p$-$3d$ and $4p$-$4s$ transitions are the same for both $4p$ states (this is partially verified by hook-method measurements of the $4p^2P_{1/2}$-$4s^2S_{1/2}$ versus $4p^2P_{3/2}$-$4s^2S_{1/2}$ oscillator-strength ratio[3,6]). With this assumption the intensity ratio of the $4p$-$3d$ versus $4p$-$4s$ lines is almost independent of which p state is radiating. In addition the photocathode sensitivity varies only a few percent between the two $4p$-$4s$ lines as well as between the three $4p$-$3d$ lines. Thus the only factor that will produce different detected intensity ratios from the different $4p^2P_J$ states is the anisotropy of the $4p^2P_{3/2}$ fluorescence. Since the Ca^+ $H=0$ and $H=50$ G ratios differed by (14±1)%, this indicated that about one-fifth of the radiation was isotropic from the $^2P_{1/2}$ state, with the remainder from the $^2P_{3/2}$ state. Thus very little ambiguity is present in the analysis of the Ca^+ ratios, while the experimental result in Table I is essentially four-fifths of the $^2P_{3/2}$-state branching ratio plus one-fifth of the $^2P_{1/2}$-state ratio.

The ratio measurements were taken with argon pressures of 0.1 to 0.4 Torr in the scattering chamber. This is insufficient density to cause transitions that could alter the branching ratios, but depolarizing collisions could decrease the anisotropy of the $^2P_{3/2}$-state decay radiation. These collisional depolarization cross sections were measured in the Hanle-effect experiments, so the size of this effect can be readily calculated and shown to produce a negligible effect on the relative anisotropy of the np-ns versus np-$(n-1)d$ decays.

The ratio uncertainties in Table I are obtained by addition of the following uncertainties: photomultiplier spectral sensitivity (5–10%), glass-filter absorption coefficients (1–2%), scatter in the data (2–3%), wavelength dependence in the detection optics (2%). One additional uncertainty arose in the Sr^+ $5p^2P_{1/2}$-state case in which the combination of branching ratio, wavelength ratio, filter absorption, and photomultiplier-sensitivity ratio produced a $5p$-$5s$ signal 240 times as large as the $5p$-$4d$ signal. As a result a leakage of as little as 4×10^{-4} of the stronger line would cause a 10% error in the ratio. Thus filter fluorescence or incomplete blocking of the stronger line could cause significant errors, as could photomultiplier nonlinearities (these and other possibilities were investigated, but they could not be entirely ruled out). It is quite likely that some such error accounts for the 20% difference between the σ^2 values reported for Sr^+ $5p^2P_{1/2}$-$4d^2D_{3/2}$ and $5p^2P_{3/2}$-$4d^2D_J$ transitions. The photomultiplier signal ratio was only 60:1 in the Sr^+ $5p^2P_{3/2}$ case, and the ratios for Ca^+ and Ba^+ were between 12:1 and 3:1. Thus *if* the reported Sr^+ $A(^2P_{1/2}$-$^2D_{3/2})/A(^2P_{1/2}$-$^2S_{1/2})$ is 25% too large due to an error associated with the large intensity ratio, then the Sr^+ $^2P_{3/2}$-state ratio might be suspected of being 6% too large from the same cause; but the Ca^+ and Ba^+ values would be erroneous by no more than 1%.

RESULTS

The directly measured results are presented in Table I; the transition probabilities deduced from these results are given in Table II. The errors in Table II are found by directly adding the percentage errors from the lifetime- and branching-ratio measurements. Thus, with the exception of the $5p^2P_{1/2}$-$4d^2D_{3/2}$ transition of Sr^+, these represent high-confidence limits and are considerably greater than standard deviations or scatter in the measurements.

No particular effort was made to obtain accurate collisional depolarization cross sections, especially in the $^2P_{1/2}$-state cases where the field dependence of the ion density produced by the discharge was a more serious problem. The general behavior of the $^2P_{3/2}$-state cross sections is found to be in order-of-magnitude agreement with theoretical expectations (Appendix III). A $J=\frac{1}{2}$ state is a unique case, since the interactions considered in the present theories lead to zero cross section in that case. Since the Sr^+ $^2P_{1/2}$-state data appear to fit a cross section of about 0.5×10^{-14} cm^2, the plausibility of such a cross section should be justified or the accuracy of the data must be questioned. Consequently, the collisional depolarization cross sections of the rubidium and cesium $^2P_{1/2}$ states in inert-gas collision have been measured. The results appear to support the validity of the Sr^+ and Ba^+ $^2P_{1/2}$-state cross sections reported here, but this cannot be definitely asserted until the theory is better understood.[12]

Our transition probability results can be compared to those of several other experiments. The Hanle-effect measurements by Bucka, Eichler, and von Oppen resulted in a linewidth 6% smaller than reported here. They measured the percentage of odd-isotope fluorescence and found nearly the 18% natural abundance. For that percentage of odd-isotope scattering and their reported linewidth, the odd-isotope correction which is

[12] Alan Gallagher (to be published).

TABLE II. Transition probabilities.

Transition	A_{exp} (10^6/sec)	f_{exp}	$\sigma_{exp}^2(ea_0)^2$	σ_{STF}^2 [a]	$\sigma_{HFDL}^2,\sigma_{HFDV}^2$ [b]	$\sigma_{B\&D}^2$ [c]
Mg^+ $3^2P_{3/2}$-$3^2S_{1/2}$	272±13	0.64±0.03	2.95±0.15	2.89		2.73
Ca^+ $4^2P_{3/2}$-$4^2S_{1/2}$	141±5	0.66±0.02	4.3±0.15	4.62	4.74, 4.45	4.30
$4^2P_{3/2}$-$3^2D_{5/2}$	7.2±0.8[d]	0.053±0.006[d]	0.25±0.03[d]	0.288	0.35, 0.095	0.24
$4^2P_{3/2}$-$3^2D_{3/2}$	0.81±0.09[d]	0.0088±0.001[d]	0.25±0.03[d]	0.288	0.35, 0.095	0.24
Sr^+ $5^2P_{3/2}$-$5^2S_{1/2}$	143±6	0.71±0.03	4.8±0.2	5.34		4.93
$5^2P_{1/2}$-$5^2S_{1/2}$	127±5	0.34±0.015	4.7±0.2	5.36		4.93
$5^2P_{3/2}$-$4^2D_{5/2}$	8.7±1.5[d]	0.096±0.02[d]	0.51±0.09[d]	0.464		0.35
$5^2P_{3/2}$-$4^2D_{3/2}$	1.0±0.2[d]	0.016±0.03[d]	0.51±0.09[d]	0.458		0.35
$5^2P_{1/2}$-$4^2D_{3/2}$	9.5±2	0.084±0.015	0.61±0.12	0.466		0.35
Ba^+ $6^2P_{3/2}$-$6^2S_{1/2}$	118±8	0.74±0.05	5.5±0.3	6.45	8.0, 4.7	5.92
$6^2P_{1/2}$-$6^2S_{1/2}$	95±7	0.35±0.025	5.6±0.4	6.53	8.1, 4.7	5.97
$6^2P_{3/2}$-$5^2D_{5/2}$	37±4[d]	0.14±0.015[d]	0.47±0.06[d]	0.454	0.55, 0.34	0.26
$6^2P_{3/2}$-$5^2D_{3/2}$	4.8±0.6[d]	0.025±0.003[d]	0.47±0.06[d]	0.436	0.53, 0.34	0.26
$6^2P_{1/2}$-$5^2D_{3/2}$	33±4	0.105±0.010	0.45±0.06	0.466	0.55, 0.34	0.27

[a] Reference 17.
[b] Hartree-Fock dipole length and dipole velocity. Reference 18 and R. H. Garstang and Stephen J. Hill, Publ. Astron. Soc. Pacific, **78**, 70 (1966).
[c] Reference 16. An extrapolation of the B&D tables to $n^*\simeq 2.4$ is required for the p-d transitions.
[d] These results were obtained from the data by assuming $\sigma^2(^2P_{3/2}\text{-}^2D_{3/2}) = \sigma^2(^2P_{3/2}\text{=}^2D_{5/2})$.

given in our Appendix I would lead to a lifetime 7 to 9% longer than the value reported here. Their approximate correction for the odd-isotope contribution gave them a lifetime $(7.0\pm0.6)\times10^{-9}$ sec as opposed to $(6.2\pm0.25)\times10^{-9}$ sec reported here. The intensity ratio fluoresced into the three decay channels from the Ba^+ $6p^2P_{3/2}$ state was also reported in Ref. 5, apparently with 90° scattered unpolarized radiation at zero magnetic field. Using the $H=0$ relative anisotropy values given here, we conclude $A(6p^2P_{3/2}\text{-}6s^2S_{1/2})/\sum_j A(6p^2P_{3/2}\text{-}5d^2D_J)=2.2$ from their intensity ratios, as opposed to 2.85±0.3 reported here. Bucka believes that this small discrepency is well within the uncertainties in their measurements (private correspondence).

In the hook-method measurements of the Ca^+, Sr^+, and Ba^+ oscillator strengths, the ion densities were established by reference to the hooks of the atom resonance lines.[3] Consequently, the result depends on the oscillator strength of the atom resonance line. Ostrovskii and Penkin use the best hook-method atomic f values to obtain $f(Ca^+\ 3933\ Å)=0.83$, $f(Sr^+\ 4078\ Å)=0.76$, $f(Ba^+\ 4554\ Å)=0.66$. If one uses the Hanle-effect results for the atomic f values,[13,14] then the Ostrovskii and Penkin data give $f(Ca^+\ 3933)=0.92$, $f(Sr^+\ 4078)=0.85$, and $f(Ba^+\ 4554)=0.69$. In view of the approximately 30% uncertainty in the hook-method results, the agreement with the values in Table II appears to be satisfactory. The ratios of oscillator strengths from the $ns^2S_{1/2}$ states can be measured more accurately by the hook method, since the vapor density of the common ground state does not cause any uncertainty. The $f(np^2P_{3/2}\text{-}ns^2S_{1/2})/f(np^2P_{1/2}\text{-}ns^2S_{1/2})$ ratios from Ref. 3 are 1.94 for Ca^+, 1.98 for Sr^+; from Ref. 6 they are 1.96 for Ca^+, 1.92 for Sr^+, and 1.98 for Ba^+; and from Ref. 15 the Ba^+ ratio is 1.98. We did not obtain the Ca^+ ratio, but the Table II ratios for Sr^+ and Ba^+ are, respectively, 2.08±0.18 and 2.12±0.30. The predictions of the Bates and Damgaard[16] and Stewart and Rotenberg[17] semiempirical theories are 2.01 for Ca^+, 2.04 for Sr^+, and 2.12 for Ba^+ (the result of almost identical σ^2 values for both transitions).

In Table II a comparison with transition probabilities from three theories has been made (additional theoretical results for Ca^+ can be found in Ref. 18, and for Mg^+ in Ref. 2). The scaled-Thomas-Fermi (STF) method of Stewart and Rotenberg[17] gives results that are within 20% of the experimental values for all but the Sr^+ $5p^2P_{1/2}$-$4d^2D_{3/2}$ transition, and as already noted the experimental value is probably at fault in that case. The STF np^2P_J-$ns^2S_{1/2}$-transition probabilities become progressively too large, going from Mg^+ to Ba^+, but otherwise no clear trends are apparent. The Bates and Damgaard (B&D) predictions for the ns-np transitions are within 8% for all four ions. This is consistent with the accuracy of the B&D method when applied to the np-ns resonance lines of the group I and II atoms. The n^* values for the $(n-1)d$ states of Ca^+, Sr^+, and Ba^+ are in the neighborhood of 2.4, so the validity of extending the B&D tables to these transitions is highly questionable. Certainly, the poor σ^2 values that result (Table II) would indicate that such an extrapolation is not a good idea. The Hartree-Fock dipole length results are generally found to be more accurate than the dipole velocity values, as is the case here. They appear to give the best results here in the cases in which they are in reasonable agreement.

ACKNOWLEDGMENTS

The work reported here is the remainder of a program started by Winthrop W. Smith and the author. Only

[13] A. Lurio, R. L. de Zafra, and R. J. Goshen, Phys. Rev. **134**, A1198 (1964).
[14] A. Lurio, Phys. Rev. **136**, A376 (1964).
[15] N. P. Penkin, Izv. Akad. Nauk SSSR, Ser. Fiz. **11**, 217 (1947).
[16] D. R. Bates and Agnete Damgaard, Trans. Roy. Soc. (London), **A242**, 101 (1949).
[17] Private correspondence. These results were calculated by Stewart following the procedure described by John C. Stewart and Manuel Rotenberg [Phys. Rev. **140**, A1508 (1965)].
[18] A. S. Douglas and R. H. Garstang, Proc. Cambridge Phil. Soc., **58**, 377 (1962).

the Ca^+ and Mg^+ Hanle-effect experiments were completed while Smith was here, but most of the problems associated with the ion Hanle-effect measurements were also solved at that time, so that much of the credit for the present results also belong to Winthrop Smith.

I would also like to thank John Hall for a number of excellent suggestions regarding optical and electronic problems.

APPENDIX I: THE HANLE-EFFECT SIGNAL FROM NATURAL BARIUM

Since 18% of natural barium is $I=\frac{3}{2}$ isotopes, a significant percentage of the natural Ba^+ resonance fluorescence will come from these odd isotopes. The $6p^2P_{3/2}$-state scattering by these odd isotopes will produce a Hanle effect of about twice the width of the $I=0$ Hanle effect, since $g_F/g_J=\frac{1}{2}$. For the experimental geometry of 90° scattering of σ radiation in the plane perpendicular to H, the Breit formula predicts a scattered intensity[10,11]

$$I_0(H)\propto 1-0.6(1+x^2)^{-1}$$

from the zero-spin isotopes, where $x=4\pi g_J\mu_0 H\tau/h$. If the nonlinear Zeeman effect is neglected, as it can be for these considerations, the Breit formula gives

$$I_{3/2}(H)\propto 1-0.19(1+x^2/4)^{-1}$$

from the $I=\frac{3}{2}$ isotopes. If the lamp had a flat spectrum, then the combined fluorescence signal would be

$$I_{\text{total}}(H)=0.82I_0(H)+0.18I_{3/2}(H).$$

If the linewidth of this signal were obtained by detecting $(d^2/dH^2)I(H)=0$, as in the present experiments, then the zeros would occur at $x=\pm(1/\sqrt{3})(1.014)$. If, as in the Bucka experiment, a fit were made to this $I(H)$ signal shape, one would obtain half-amplitude points between $x=\pm1.02$ and ±1.04 depending on how heavily the wings were weighted ($[I(\infty)-I(x)]/[I(\infty)-I(0)]=\frac{1}{2}$ occurs at $x=\pm1.04$). Thus the difference between the $I=0$ linewidth and the natural barium linewidth would be 1.4% with modulation detection and 2–4% for dc detection if 18% of the scattering were from the $I=\frac{3}{2}$ isotopes. These differences will scale almost linearly with the actual amount of $I=\frac{3}{2}$ scattering as long as it does not exceed the amount of $I=0$ scattering.

In the case of the Ba^+ $6p^2P_{1/2}$ state, $|g_F/g_J|=\frac{1}{4}$ for the $I=\frac{3}{2}$ isotopes, and an equivalent analysis for this case shows that the odd-isotope scattering will produce $\frac{1}{4}$ as much broadening of the $I=0$ width as in the $6p^2P_{3/2}$ case.

APPENDIX II: SCATTERED INTENSITY RATIO VERSUS BRANCHING RATIO

To calculate the ratio of the intensities fluoresced into different decay channels from a common optically excited state, we can use the Breit formula, but the k^4 factors, which differ for the different decay channels, must be kept outside of the usual proportionality factors.[19] Specifically, we use for the intensity radiated into a solid angle $d\Omega$

$$R_\alpha(f,\bar{g})=Cd\Omega\sum_{m,\mu,\mu',m'}\frac{f_{\mu m}f_{m\mu'}g_{\mu' m'}g_{m'\mu}}{1+2\pi i\tau\Delta E_{\mu\mu'}/h}k_\alpha{}^4, \quad (1)$$

where $R_\alpha(\bar{f},\bar{g})$ is the intensity of radiation with wave number k_α (i.e., the radiation from the decay transitions to the Zeeman levels m' of the final state α).

The coefficient C, which is common to all the $R_\alpha(\bar{f},\bar{g})$, contains all factors such as the vapor density that are common to the rate of excitation. The remaining symbols are defined as in Ref. 11. Since these are single electron spectra, the transition probability A is given by

$$A_\alpha\equiv A(np^2P_J\rightarrow\alpha)=\frac{64\pi^4}{3h}k_\alpha{}^3\frac{2J+1}{2J_\alpha+1}\zeta(J,J_\alpha)\times(np^2P_J:r:\alpha)^2.$$

Thus the reduced matrix elements in the $g_{\mu' m'}g_{m'\mu}$ can be combined with $k_\alpha{}^3$ to give

$$R_\alpha=\frac{Cd\Omega k_\alpha A_\alpha}{\zeta(J,J_\alpha)}\frac{2J_\alpha+1}{2J+1}\sum\frac{f_{\mu m}f_{m\mu'}g'_{\mu' m'}g'_{m'\mu}}{1+2\pi i\tau\Delta E/h} \quad (2)$$

where $g'_{\mu' m'}=g_{\mu' m'}/(n^2P_J;\,r;\,\alpha)$ contains only the angular parts of the decay matrix elements. For unpolarized incident and detected radiation the sums in Eq. 2 must be separately evaluated for each pair of incident and radiated polarization modes, and the results added. For the present case of 90° scattering in the plane perpendicular to H, $n^2S_{1/2}$ ground state, $n^2P_{3/2}$ excited state, and $n^2S_{1/2}$, $(n-1)^2D_{3/2}$, or $(n-1)^2D_{5/2}$ final states (labeled $\alpha=1,2,3$, respectively), we obtain

$$\frac{R_3+R_2}{R_1}=\frac{k_3A_3[162-6/(1+x^2)]+k_2A_2[152+24/(1+x^2)]}{k_1A_1[170-30/(1+x^2)]}. \quad (3)$$

With the assumption that $\sigma^2(np^2P_{3/2}\rightarrow 2)=\sigma^2(np^2P_{3/2}\rightarrow 3)$, the following indentifications can be made:

$$A_3=\frac{A_2+A_3}{1+(k_2/k_3)^3/9},\quad A_2=\frac{A_2+A_3}{1+9(k_3/k_2)^3}.$$

APPENDIX III: ION-ATOM COLLISIONAL DEPOLARIZATION

The collisional depolarization cross sections for ion excited states in collisions with atoms can be calculated

[19] E. U. Condon and G. H. Shortley, *The Theory of Atomic Spectra* (Cambridge University Press, London, 1959), p. 90.

using the methods of Byron and Foley,[7] Omont,[8] or D'Yakonov and Perel.[9] To outline the necessary extension of these theories of atom-atom collisions, we follow the method of Omont. The impact approximation and perturbation theory (to second order) relate the collisional depolarization cross section to $\Delta\rho$, the change in the density matrix of one pair of colliding atom and ion due to a single collision. This $\Delta\rho$ is found from Eqs. (6), (17), and (26) of Ref. 8, which we repeat here:

$$\Delta\rho = A\rho(-\infty)A^{+} - \rho(-\infty), \tag{4}$$

where

$$A_{pq}{}^{p'q'} = \exp\left\{-i\int_{\infty}^{\infty} dt\left[\langle pq|V|p'q'\rangle + \frac{\langle pq|V|p''q''\rangle\langle p''q''|V|p'q'\rangle}{\Delta E}\right]\right\}, \tag{5}$$

and

$$\Delta E_{pq,p'q'} \ll 1/\tau_{\text{collision}} \ll \Delta E_{pq,p''q''}. \tag{6}$$

Here $V(b,v,t)$ is the collisional interaction; and in the present case p, p', p'' represent ion electronic states while q, q', q'' are atom electronic states. The expansion of the ion-atom electrostatic interaction gives for V:

$$V = -\frac{q\mathbf{P}_A\cdot\hat{R}}{R^2} + \frac{3q\hat{R}\cdot\mathbf{D}_A\cdot\hat{R}}{R^3} + \frac{3\mathbf{P}_I\cdot\hat{R}\mathbf{P}_A\cdot\hat{R} - \mathbf{P}_I\cdot\mathbf{P}_A}{R^3} + \frac{6\mathbf{P}_A\cdot\mathbf{D}_I\cdot\hat{R} - 15\mathbf{P}_A\cdot\hat{R}\hat{R}\cdot\mathbf{D}_I\cdot\hat{R}}{R^4} - \frac{6\mathbf{P}_I\cdot\mathbf{D}_A\cdot\hat{R} - 15\mathbf{P}_I\cdot\hat{R}\hat{R}\cdot\mathbf{D}_A\cdot\hat{R}}{R^4} + \cdots. \tag{7}$$

Here q is the excess ion charge, $\mathbf{P}_I$, $\mathbf{D}_I$, $\mathbf{P}_A$, $\mathbf{D}_A$ are the ion and atom dipole and quadrupole operators, $\mathbf{R}$ is the internuclear vector, and we will label the five terms on the right V_1 to V_5, respectively, in the following discussion.

In the case of n^1S_0 ground-state atoms, Eq. 6 requires that $q=q'=n^1S_0$ and that p and p' must be sublevels of the initial ion excited state. In this case, which includes the present experiments, $\langle pq|V|p'q'\rangle = 0$ in Eq. 5. It is worth noting, however, that if the atom does not have a $^1S_0$ ground state, then $\langle pq|V_2|p'q'\rangle \neq 0$ is possible, but since V_2 involves only the atom electronic coordinates, $\langle qp|V_2|p'q'\rangle$ is diagonal in pp' and independent of p. Thus this interaction does not produce any change in the density matrix of the ion and it does not contribute to the depolarization cross section. Considering now the $\langle V\rangle\langle V\rangle/\Delta E$ contribution to Eq. 5, the largest term will be $\langle V_1\rangle\langle V_1\rangle/\Delta E$, which represents the polarization of the atom by the excess charge of the ion. Since V_1 does not involve the ion electronic coordinates, this interaction will also produce no change in the ion density matrix. The next-largest nonzero terms are $\langle V_3\rangle\langle V_3\rangle/\Delta E$ and $\langle V_1\rangle\langle V_4\rangle/\Delta E$. These are both R^{-6} interactions involving comparable magnitudes of energy denominators and valence-electron matrix elements. The $\langle V_3\rangle\langle V_3\rangle/\Delta E$ term is the dipole-dipole interaction responsible for nonresonant atom-atom depolarization, so it can be seen that the cross sections for ion-atom collisions should be found quite generally to be the same magnitudes as those nonresonant atom-atom collisions. This was found to be the case in the present experiments. Other long-range contributions to the cross sections may be significant but should not alter the magnitudes (e.g., the $\langle V_1\rangle\langle V_3\rangle\langle V_3\rangle\langle V_1\rangle$ which appears in fourth-order perturbation theory and represents the interaction of the ion with an atom polarized by the Coulomb field of the ion).

The present theories for atom-atom collisions cannot be used directly for highly-excited states, and the same restrictions apply to the present arguments. Also, a $J=\frac{1}{2}$ state has unique properties in atom-atom collisions as well as ion-atom collisions, so for the present experiments this discussion applies only to the $np^2P_{3/2}$ states.[12]